



Thermal properties of simulated Hanford waste glasses

Journal:	<i>Journal of the American Ceramic Society</i>
Manuscript ID	JACERS-38354
Manuscript Type:	Article
Date Submitted by the Author:	21-Mar-2016
Complete List of Authors:	Rodriguez, Carmen; Pacific Northwest National Laboratory, Material Science Chun, Jaehun; Pacific Northwest National Laboratory, Experimental Fluid Mechanics Crum, Jarrod; Pacific Northwest National Laboratory, Glass and Materials Science Team Canfield, Nathan; Pacific Northwest National Laboratory, Fuel Cells Rönnebro, Ewa; Pacific Northwest National Laboratory, Applied Functional Materials Vienna, John; Pacific Northwest National Laboratory, Glass Development Laboratory Kruger, Albert; U.S. Department of Energy, Office of River Protection
Keywords:	nuclear waste, glass, thermal properties

SCHOLARONE™
Manuscripts

view

Thermal properties of simulated Hanford waste glasses

Carmen P. Rodriguez^{a*}, Jaehun Chun^a, Jarrod V. Crum^a, Nathan L. Canfield^a, Ewa Ronnebro^a,

John D. Vienna^a and Albert A. Kruger^b

^a*Pacific Northwest National Laboratory, Richland, WA 99352, USA*

^b*U.S. Department of Energy, Office of River Protection, Richland, WA 99352, USA*

ABSTRACT

The Hanford Tank Waste Treatment and Immobilization Plant (WTP) will vitrify the mixed hazardous wastes generated from 45 years of plutonium production. The molten glasses will be poured into stainless steel containers or canisters and subsequently quenched for storage and disposal. Such highly energy-consuming processes require precise thermal properties of materials for appropriate facility design and operations. Key thermal properties (heat capacity, thermal diffusivity, and thermal conductivity) of representative high-level and low-activity waste glasses were studied as functions of temperature in the range of 200 to 800°C (relevant to the cooling process), implementing simultaneous differential scanning calorimetry–thermal gravimetry (DSC-TGA), Xe-flash diffusivity, pycnometry, and dilatometry. The study showed that simultaneous DSC-TGA would be a reliable method to obtain the heat capacity of various glasses in the temperature range of interest. Accurate thermal properties from this study were shown to provide a more realistic guideline for capacity and time constraints of the heat removal process, in comparison to the design basis conservative engineering estimates. The estimates, though useful for design in the absence of measured physical properties, can now be supplanted and the measured thermal properties can be used in design verification activities.

Keywords: Nuclear waste glasses, Cooling process, Heat capacity, Heat conductivity

* Corresponding author. Tel.: +1 509 375 2464; fax: +1 509 372 5997.
E-mail address: carmen.rodriguez@pnnl.gov (C.P. Rodriguez).

INTRODUCTION

The Hanford Site in southeastern Washington State has one of the largest concentrations of radioactive wastes in the world. The waste is the legacy of 45 years of plutonium production for nuclear weapons, beginning with the Manhattan project in the 1940s.¹ Approximately 56 million gallons of high-level waste (HLW) and low-activity waste (LAW) are stored in 177 underground tanks near the Columbia River at the Hanford site in Washington State. The Hanford Tank Waste Treatment and Immobilization Plant (WTP) is being constructed to treat the wastes via vitrification, and once immobilized in a glass form they will be destined for disposal.² The WTP includes a pretreatment facility to separate the wastes into a small volume of HLW containing a large fraction of the radioactive isotopes of concern and a large volume of LAW fraction. Subsequent to pretreatment, vitrification takes place in liquid-fed, ceramic-lined, Joule-heated melters (at $\sim 1150^{\circ}\text{C}$).³ During this process, radioactive elements are incorporated into the glass structure, producing a durable glass form that can isolate the radioactive isotopes from the environment for hundreds of thousands of years.⁴

The last step of the WTP vitrification process involves pouring of molten glass, produced in the melter, into canisters or containers for immobilized HLW/LAW, where it cools. In the WTP, the canisters/containers are filled and cooled inside a small room, called the pour cave. The pouring leads to asymmetrical and transient heat transfer inside the pour cave. The heat contained in the molten glass must be removed from the containers without slowing the plant process. The total amount of heat to be removed and the heat release rate depend on the thermal properties of the glass, which will vary as the glass composition changes. Furthermore, the release rate also depends on the local environment, which includes other hot canisters/containers.⁵⁻⁷

While there have been many studies on thermal properties of glasses, very limited studies have been performed for nuclear waste glasses.⁸ Such limited studies showed significant

1 uncertainties in the thermal properties owing to difficulties involved in experimental
2 measurements.⁸ These properties are crucial inputs for heat load calculations to assess the ability
3 of the heating, ventilation, and air conditioning (HVAC) system of the WTP to meet the current
4 facility design basis as to heat load; as a result, the properties can be a basis to affect or modify
5 the design of the HVAC system of the WTP.⁹
6
7
8
9
10

11 In this study, we determined the heat capacity and thermal conductivity (through thermal
12 diffusivity and density) of representative HLW and LAW glasses as functions of temperature, by
13 using a combination of simultaneous differential scanning calorimetry–thermal gravimetry
14 (DSC-TGA) (heat capacity), Xe-flash diffusimeter (thermal diffusivity), and
15 pycnometry/dilatometry (density). As will be clearly shown, the applied techniques help alleviate
16 the uncertainties involved in the measurements of thermal properties of the HLW and LAW
17 glasses. In the next section, background information is provided along with a brief discussion of
18 the experimental methods used in this study. Measured thermal properties are then presented,
19 followed by a discussion of their impacts on WTP facility design.
20
21
22
23
24
25
26
27
28
29
30
31
32
33
34
35

36 BACKGROUND

37 Numerical models have been developed to predict a temperature distribution within the glass
38 and heat emitted from the containers/canisters during cooling.^{5, 6} The key parameters for
39 estimating the heat load from cooling glass are the glass heat capacity or specific heat (C_p),
40 thermal conductivity (k), and density (ρ) as functions of temperature. The specific heat is the heat
41 required per unit mass of material to increase its temperature by one unit. The thermal
42 conductivity of a material is defined via the heat flux (a rate of heat transfer per unit area, q)
43 through the material that is subjected to a temperature gradient (∇T): $q = -k\nabla T$ (Fourier's law),
44 where T denotes temperature.
45
46
47
48
49
50
51
52
53
54
55
56
57
58
59
60

1 The thermal diffusivity (α) is a measure of how fast the material can conduct thermal energy,
2
3 in comparison to its ability to store thermal energy. It is defined as
4

$$\alpha = \frac{k}{\rho C_p}. \quad (1)$$

5
6
7
8
9 The heat transfer equation in a solid without heat sources or sinks is¹⁰

$$\rho C_p \frac{\partial T}{\partial t} = -k \nabla T \quad (2)$$

11
12
13
14
15
16 where t denotes time. Typically, heat capacity and thermal diffusivity have been measured by
17
18 steady-state alternating current (AC) calorimetry¹¹ or flash thermal diffusivity.¹²⁻¹⁴ Thermal
19
20 conductivity can be calculated from Eq. (1). The density is generally obtained using pycnometry
21
22 and dilatometry.
23
24
25
26

27 **EXPERIMENTAL**

28 *Glass Compositions*

29
30
31
32 Table 1 shows the simulated glass compositions used in this study: LAWB99, LAWA44,
33
34 ORPLA20 and ORPLD1 are simulated LAW glasses, and HLW-Ng-Fe2, HLW-E-Al-27 and
35
36 WTP-C106 are simulated HLW glasses. These glasses were formulated and corresponding large-
37
38 scale melter tests have been performed at The Catholic University of America.¹⁵⁻¹⁷ These seven
39
40 glasses were selected from a large database of potential Hanford waste glasses to represent the
41
42 range of compositions likely to be produced in either the LAW or HLW vitrification plants:
43
44 WTP LAW glasses with high soda (ORPLA20), intermediate soda (LAWA44 and ORPLD1),
45
46 and lower soda (LAWB99); HLW glasses with high iron (HLW-Ng-Fe2), high alumina (HLW-
47
48 Al-27), and an intermediate composition (WTP-C106). Table 1 also includes compositions of
49
50 two Japanese simulated HLW glasses (Sugawara A and B) that were used as reference glasses
51
52 because of their well-characterized thermal properties.¹⁸ All glasses were batched and melted
53
54 following the glass batching and melting procedure described by Schweiger et al.¹⁹ Molten glass
55
56
57
58
59
60

1 was poured into bars (13 × 13 × 50 mm) that were annealed at each glass transition temperature
2
3 for one hour and then cooled to room temperature at 1°C/min. The annealed glass bars were used
4
5 to prepare samples for heat capacity, density, and thermal diffusivity measurements. In order to
6
7 obtain reliable thermal properties, the aforementioned sample preparation procedure was
8
9 maintained to minimize possible variations of the properties.
10
11

12 *Specific Heat or Specific Heat Capacity*

13
14
15 Simultaneous DSC-TGA (STA 449 F1 Jupiter® with an automatic sample carrier) was used
16
17 to measure C_p . The system employed for this work was equipped with a silicon carbide furnace.
18
19 Helium was used as both a purge and protective gas at a constant flow rate of 35 mL/min. The
20
21 specific heat of the glass was determined based on three repeating measurements: baseline,
22
23 sapphire (standard), and sample. All these measurements were conducted under constant heating
24
25 and cooling rates of 20°C/min using identical crucibles and conditions.
26
27
28
29
30

31 Samples were prepared with a specific procedure to achieve optimum and reliable results.
32
33 The annealed bar was placed into an epoxy mold. Using a 0.25 inch (6.35 mm) diamond core-
34
35 drilling saw, a cylindrical glass core with a diameter of 0.247 inches (6.27 mm) was removed.
36
37 1.2 mm thick disks were cut from the core by a Buehler Isomet low-speed saw with a low-
38
39 concentration diamond wafering blade. The disks were flattened and polished to a thickness of
40
41 ~1.0 mm using a grinder and polisher (LECO SS-200).
42
43
44

45 In the experiment, the baseline reproducibility was checked by measuring an empty crucible
46
47 (platinum crucible, 0.085 ml, NETZSCH NIB005508) three times. The first run was used to burn
48
49 off any impurities and residues from the crucibles, followed by two more runs with an empty
50
51 crucible. To check the reproducibility, accuracy, and calibration of the simultaneous DSC-TGA,
52
53 two measurements were conducted using a 1 mm thick sapphire disk (Order No. 6.235.1-91.100,
54
55 NETZSCH) and then the sample measurement was performed afterward. All of these six
56
57
58
59
60

1
2
3
4
5
6
7
8
9
10
11
12
13
14
15
16
17
18
19
20
21
22
23
24
25
26
27
28
29
30
31
32
33
34
35
36
37
38
39
40
41
42
43
44
45
46
47
48
49
50
51
52
53
54
55
56
57
58
59
60

measurements were performed using the same crucible. The temperature program sequence employed for these measurements was as follows:

1. initial isothermal segment of 25 min at 100°C recommended to stabilize the starting temperature;
2. dynamic segment up to 850°C with a heating rate of 20°C/min to maximize signal and minimize the influence of small shifts in baseline;
3. isothermal segment of 35 min at 850°C;
4. dynamic segment with a cooling rate of 20°C/min down to 100°C; and
5. isothermal segment of 35 min at 100°C as a final step.

This procedure was repeated for each glass. For better accuracy and reproducibility, the crucibles were placed at exactly the same position during all the measurements, which was achieved by the auto sampler.

Density at Ambient Temperature

The densities of glass samples were determined by gas displacement using a helium pycnometer (AccuPyc II 1340). It measures the displaced volume of helium gas occupied by the sample. Combining the volume of a solid with its mass allows for an accurate determination of a material's true density. After the gas pycnometer's warm-up period, it was calibrated using a spherical metal calibrated volume standard. Subsequently, a small glass sample was placed into the pycnometer chamber. The density was measured according to a technical procedure described elsewhere.^{20, 21}

Thermal Expansion

The linear coefficient of thermal expansion (CTE), defined by the amount of expansion ($\Delta L/L$, where L is the initial length and ΔL is the change in length) for a unit temperature change,

1 was measured using a Linseis L75 platinum series single-rod vertical dilatometer configured
 2 with an alumina measuring head. The dilatometer was prepared for measurements by running an
 3 alumina sample three times to determine the average background expansion of the instrument.
 4
 5 The three runs were used to subtract the instrument's background expansion as a function of
 6
 7 temperature. Subsequently, NBS 732 (borosilicate glass, National Institute of Standards and
 8
 9 Technology standard reference material) was measured to confirm reliable operation of the
 10
 11 dilatometer for CTE over the temperature range of interest. After the verification, the HLW,
 12
 13 LAW, and Sugawara glass Sample A and B bars all cut to $\sim 25 \times 3 \times 3$ mm were heated at
 14
 15 $1^\circ\text{C}/\text{min}$ from 25°C to the softening point. The software automatically terminated the ramp
 16
 17 heating once the sample exceeded the glass softening point (determined by onset of shrinkage).
 18
 19 The CTE was calculated relative to 25°C for temperatures below glass transition temperature, T_g .
 20
 21
 22
 23
 24
 25
 26
 27
 28

29 ***Density at Elevated Temperature***

30
 31 The CTE and density at ambient temperature (*i.e.*, 25°C) were used to calculate the density of
 32
 33 each glass as a function of temperature using the following expression:
 34
 35
 36
 37
 38

$$39 \quad \rho_t = \frac{\rho_0}{[1 + 3\alpha_t(T_t - T_0)]} \quad (3)$$

40
 41 where

42
 43 ρ_t = density at temperature T_t

44
 45 ρ_0 = density at 25°C

46
 47 α_t = CTE at temperature T_t

48
 49 T_t = temperature, $^\circ\text{C}$

50
 51 T_0 = ambient temperature, 25°C
 52
 53
 54
 55
 56
 57
 58
 59
 60

1 Note that the numerical factor 3 was used to convert linear expansion CTE to volume expansion
2 based on the assumption that an initial volume of the sample can be approximated by L^3 .
3
4
5
6

7 *Thermal Diffusivity*

8
9 Measurements of thermal diffusivity were collected with a Xe-flash diffusimeter (Anter
10 Corporation Flashline 2000). Measurements were performed with a 50°C interval from room
11 temperature to 400°C, below T_g of the glasses. Samples of annealed glass were core-drilled and
12 machined with diamond impregnated tooling to a diameter of 12.6 mm. Subsequently, the disks
13 were cut with a diamond impregnated blade. The disks were then ground and polished with a
14 series of SiC sandpaper grits to a finish of 1200 grit and final thickness between 0.5 and 2 mm.
15 These samples were coated on top and bottom with ~1200 nm of Au using an e-beam deposition
16 system. Lastly, graphite (supplied by Anter) was sprayed onto the top and bottom surfaces to
17 maximize absorption of the xenon flash. The combination of Au and graphite was used to ensure
18 that the energy from the flash was absorbed at the surface of the sample, and further reduce
19 reflection of the light/energy or incongruent diffusion of the energy into the bulk of the glass.
20
21
22
23
24
25
26
27
28
29
30
31
32
33
34
35
36
37

38 *Thermal Conductivity*

39 For the one-dimensional situation, where the temperature gradient is (dT/dx) , thermal
40 conductivity is given by:
41
42
43

$$44 \quad q = -k (dT/dx) \quad (4)$$

45
46
47 The k value [W/m·K] was calculated using Eq. (1).
48
49
50
51

52 **RESULTS AND DISCUSSION**

53 *Specific Heat*

54
55 As described, C_p of the sample was determined by conducting three different sets of
56 measurements (i.e., empty crucible, sapphire, and sample) at a constant heating rate. The first set,
57
58
59
60

1 including three baseline measurements with an empty crucible, were carried out for each glass as
2 shown in Figure 1(a). The heating and cooling segments of the DSC curves show good
3 reproducibility with the exception of a small reaction around 100°C in the first measurement, due
4 to the burn-off of impurities and/or residues of the empty crucible.
5
6
7
8

9 The second set of measurements was performed with a standard material (*i.e.*, sapphire)
10 whose specific heat is known.²² Figure 1(b) shows three different sapphire DSC heating and
11 cooling curves, which indicates the reproducibility of the DSC-TGA for specific heat
12 measurements. The specific heat of the sapphire standard was plotted versus measured sapphire
13 values, as shown in Figure 2. This clearly suggests that the DSC-TGA is a reliable method to
14 obtain the specific heat of the glass samples.
15
16
17
18
19
20
21
22
23

24 The C_p values of four LAW glass formulations (LAWA44, ORPLA20, ORPLD1, and
25 LAWB99), three HLW glass formulations (HLW-NG-Fe2, HLW-E-Al-27, and WTP-C106) and
26 two Japanese simulated HLW glass formulations (Sugawara A and B) were evaluated.¹⁸ Each
27 sample was measured three times. The average C_p values of the cooling segment of the LAW,
28 HLW, and Japanese glasses are shown in Figures 3–5, respectively. Based on all of the data, the
29 overall trend suggests that C_p is nearly constant above ~550°C. The C_p was obtained from the
30 cooling segment because the heating segment displays unreproducible peaks due to
31 crystallization around the glass transition temperature. This is based on the experimental
32 observations for the measurements with sapphire, in which the measurement from the cooling
33 segment shows the lowest uncertainty (0.11% of standard deviation) in comparison to those from
34 the heating and isothermal segments (0.64% and 0.77% of standard deviation, respectively), as is
35 shown in Figure 1(b). Values of C_p for the LAW glasses between the glass transition temperature
36 and 800°C range from 1500 J/(kg·K) to 1600 J/(kg·K). This range is comparable to that of the
37 HLW glasses but is slightly lower than that of the HLW glasses (1580–1650 J/(kg·K)) over the
38 same temperature range.
39
40
41
42
43
44
45
46
47
48
49
50
51
52
53
54
55
56
57
58
59
60

1
2
3
4
5
6
7
8
9
10
11
12
13
14
15
16
17
18
19
20
21
22
23
24
25
26
27
28
29
30
31
32
33
34
35
36
37
38
39
40
41
42
43
44
45
46
47
48
49
50
51
52
53
54
55
56
57
58
59
60

Figure 5 shows the C_p values of the two Japanese simulated HLW glasses (Sugawara A and Sugawara B) from our measurements, along with data from Sugawara et al.¹⁸ (Sample A and Sample B). Note that Sugawara A is the same as Sample A and Sugawara B is the same as Sample B (i.e., independent measurements for the identical samples). The C_p values for corresponding identical samples (i.e., Sugawara A with Sample A and Sugawara B with Sample B) are very similar over the temperature range from 200°C to 800°C, which supports the accuracy of our measurements.

Density

The density, measured by gas pycnometry at ambient temperature, of all the samples ranged from 2544.1 up to 2739.9 kg/m³, as is shown in Tables 2, 3, and 4. The density as a function of temperature was calculated using measured linear CTEs and plotted for all the glasses, as shown in Figure 6. The densities decrease with increasing temperature in a nearly linear fashion to minima of 2511.2 to 2703.5 kg/m³ near T_g for the samples. Densities were not calculated for temperatures above T_g . High temperature densities for LAWA44, ORPLA20, HLW-E-AI-27, and WTP-C106 are available in Gan et al.²³

Thermal Diffusivity

Thermal diffusivities are plotted versus temperature in Figure 7, with specific values given in Tables 2, 3, and 4, in the range of 25°C to 400°C. Thermal diffusivities of the samples are the highest at 25°C and decrease as temperature increases in a nearly linear fashion. The thermal diffusivities of the HLW glasses measured are similar to each other: $4.3\text{--}4.6 \times 10^{-7}$ m²/s at 25°C and 3.9×10^{-7} m²/s at 400°C. Sugawara A and B had similar diffusivities: $4.3\text{--}4.7 \times 10^{-7}$ m²/s at 25°C and $3.8\text{--}4.2 \times 10^{-7}$ m²/s at 400°C. For the LAW glasses, thermal diffusivities of ORPLA20 and ORPLD1, ranging from 3.9×10^{-7} to 4.2×10^{-7} m²/s, are similar to those of the HLW

1 glasses. LAWB99 and LAWA44 have higher diffusivities ($4.9\text{--}5.2 \times 10^{-7} \text{ m}^2/\text{s}$ at 25°C and 4.7--
2 $4.9 \times 10^{-7} \text{ m}^2/\text{s}$ at 400°C) than other glasses measured at all temperatures. Thermal diffusivities
3 of all LAW glasses between 100°C and 200°C are not quite as linear as the rest of the data
4 points. There is no clear physical phenomenon associated with this behavior and data are being
5 currently investigated to determine whether this is an experimental artifact. However, this is not
6 expected to have any impact on the use of these data to support a more rigorous engineering
7 analysis of the HVAC system for each of the vitrification facilities.
8
9
10
11
12
13
14
15
16
17
18

19 ***Thermal Conductivity***

20 Thermal conductivities were calculated from 25°C up to 400°C for all the glasses using
21 measured diffusivities, densities, and specific heats, as shown in Eq. (1) (see Tables 2, 3, and 4
22 for detailed values). All thermal conductivity values are within a range of known thermal
23 conductivities (*i.e.*, 0.8 to $2.18 \text{ W/m}\cdot\text{K}$) for common commercial glasses found in previous
24 studies.²⁴⁻²⁷ Figure 8 shows thermal conductivities of the samples in the range of 25 to 400°C and
25 corresponding linear regressions fit to the data. The linear regressions show strong linear trends
26 (typically, $R^2 > 0.94$), indicating a good linear relationship between thermal conductivity and
27 temperature over the range tested. Intercepts (at 0°C) for the fits ranged from 0.93 to 1.20
28 $\text{W/m}\cdot\text{K}$ and slopes ranged from 4.0×10^{-4} to $10.0 \times 10^{-4} \text{ W/m}\cdot\text{K}$. Note that the data at $\sim 400^\circ\text{C}$ for
29 some samples shows slight deviations from the linear regression because the measured properties
30 (C_p , CTE, and α) are slightly influenced by the glass transition behavior near T_g .
31
32
33
34
35
36
37
38
39
40
41
42
43
44
45
46
47

48 The thermal conductivities measured in this study (25 to 400°C) are plotted beside existing
49 high temperature (800 to 1150°C) values (labeled “*” in the key) measured by Gan et al.²³ in
50 Figure 9. Combined, these data cover the temperature ranges of interest.
51
52
53
54
55
56
57
58
59
60

SUMMARY AND IMPLICATIONS

Key thermal properties of four LAW, three HLW, and two Japanese simulated waste glasses were determined as a function of temperature by using simultaneous DSC-TGA (heat capacity), Xe-flash diffusivity (thermal diffusivity), pycnometry (density at ambient temperature), and dilatometry (thermal expansion).

The simultaneous DSC-TGA was shown to provide a reliable and reasonable C_p of various glasses in the temperature range of interest. The C_p values of these nine glasses are relatively close and follow the same trend; the LAW glasses showed slightly lower C_p than the HLW glasses, and two Japanese simulated HLW glasses (Sugawara A and B) showed higher C_p values than those of LAW and HLW glasses. A combination of ρ at room temperature and CTE measurement from 25°C up to T_g enabled us to determine the variation of the glass density as a function of temperature. The Xe-flash diffusivity measurements gave rise to α values of selected HLW and LAW glasses from 25°C up to 400°C; α values are inversely proportional to temperature. Correlating α with C_p and ρ , values of k were determined from 25°C up to 400°C for two HLW and two LAW glasses and one glass from the literature. All the measured k values were within the expected range for glass.

Accurate thermal properties data is key information for design and operation of heat removal processes in the WTP. Measured C_p values are compared to the bounding values used in previous plant design activities in Figure 10. It is clear from this comparison that the total heat removed by cooling LAW melt and glass is significantly less than the conservative estimates across the entire temperature range. Such difference implies that a more rigorous engineering analysis of the HVAC system can be performed for each of the vitrification facilities; the analysis will contribute to projections of operation efficiencies for both HLW and LAW facilities. Furthermore, the analysis can affect the design and implementation of advanced melters; while

1 current generation melters are designed to produce 15 MT glass/day, the advanced melters can
2 produce up to 50 MT glass/day.
3
4
5
6

7 **ACKNOWLEDGEMENTS**

8
9
10
11 This work was funded by Federal Project Director William F. Hamel, Jr. of the
12 Department of Energy's Hanford Tank Waste Treatment and Immobilization Plant. The proposal
13 for this effort was submitted by Albert A. Kruger and Ricky Bang as an entry to the 2013 U.S.
14 Department of Energy Office of River Protection (ORP) Grand Challenge. The authors are
15 grateful to Michael J. Schweiger and Ekkehard Post for insightful discussions and instructions on
16 the TGA-GC-MS setup and tests, respectively. Pacific Northwest National Laboratory is
17 operated by Battelle Memorial Institute for the U.S. Department of Energy under contract DE-
18 AC05-76RL01830.
19
20
21
22
23
24
25
26
27
28
29
30
31
32

33 **References**

- 34
35
36
37
38 1. R. E. Gephart, "A Short History of Hanford Waste Generation, Storage, and Release,"
39 PNNL-13605, Rev. 4, Pacific Northwest National Laboratory, Richland, WA, 2003.
40
41
42 2. DOE, "Design, Construction, and Commissioning of the Hanford Tank Waste Treatment
43 and Immobilization Plant," U.S. Department of Energy, Office of River Protection,
44 Richland, WA, 2000.
45
46
47
48 3. J. D. Vienna, "Nuclear Waste Vitrification in the United States: Recent Developments
49 and Future Options," *International Journal of Applied Glass Science* **1** [3] 309-321
50 (2010).
51
52
53
54
55
56
57 4. B. Grambow, "Nuclear waste glasses - How durable?" *Elements* **2** [6] 357-364 (2006).
58
59
60

- 1
2
3
4
5
6
7
8
9
10
11
12
13
14
15
16
17
18
19
20
21
22
23
24
25
26
27
28
29
30
31
32
33
34
35
36
37
38
39
40
41
42
43
44
45
46
47
48
49
50
51
52
53
54
55
56
57
58
59
60
5. D. P. Guillen, "Thermal Predictions of the Cooling of Waste Glass Canisters," Idaho National Laboratory (INL), Idaho Falls, Idaho, 2014.
6. K. J. Knight, J. Berkoe, B. Rosendall, J. Peltier and C. Kennedy, "Applying Fluid Dynamics Simulations to Improve Processing and Remediation of Nuclear Waste," in *ASME 2011 14th International Conference on Environmental Remediation and Radioactive Waste Management*, American Society of Mechanical Engineers, 2011.
7. C. Barringer, J. Berkoe, C. Rayner, and G. Huang, "Application of Computational Fluid Dynamics in the Simulation of a Radioactive Waste Vitrification Facility," in *ASME 2004 Heat Transfer/Fluids Engineering Summer Conference*, American Society of Mechanical Engineers, 2004.
8. H. Gan, F. Perez-Cardenas, and I. L. Pegg. "Literature Survey on Glass Physical Properties for LAW Container Fill Model," VSL-99R3610-1, Rev. 0, Aug. 26, 1999, Publically Released as ORP-59676, 2016.
9. A. A. Kruger, et al., "Crystal Settling, Redox, and High Temperature Properties of ORP HLW and LAW Glasses," VSL-09R1510-1, Vitreous State Laboratory, The Catholic University of America, Washington, D.C., 2015.
10. R. B. Bird, W. E. Stewart, and E. N. Lightfoot, *Transport Phenomena*, John Wiley & Sons, New York, 1960.
11. G. Yang, A. D. Migone, and K. W. Johnson, "Heat capacity and thermal diffusivity of a glass sample," *Physical Review B* **45** [1] 157 (1992).
12. J. Chiguma, E. Johnson, P. Shah, N. Gornopolskaya, and W. E. Jones, Jr., "Thermal Diffusivity and Thermal Conductivity of Epoxy-Based Nanocomposites by the Laser Flash and Differential Scanning Calorimetry Techniques," *Open Journal of Composite Materials* **3** [3] 12 (2013).
13. T. Kabayabaya, F. Yu, and X. Zhang, "Thermal diffusivity measurement of glass at high temperature by using flash method." *Journal of Thermal Science* **13** [1] 91-96 (2004).

- 1
2
3
4
5
6
7
8
9
10
11
12
13
14
15
16
17
18
19
20
21
22
23
24
25
26
27
28
29
30
31
32
33
34
35
36
37
38
39
40
41
42
43
44
45
46
47
48
49
50
51
52
53
54
55
56
57
58
59
60
14. W. J. Parker, R. J. Jenkins, C. P. Butler, and G. L. Abbott, "Flash method of determining thermal diffusivity, heat capacity, and thermal conductivity." *Journal of Applied Physics* **32** [9] 1679-1684 (1961).
 15. I. S. Muller, et al., "Compilation and Management of ORP Glass Formulation Database." VSL-12R2470-1, Vitreous State Laboratory, The Catholic University of America, Washington, D.C., 2012.
 16. G. F. Piepel, S. K. Cooley, I. Muller, H. Gan, I. Joseph, and I. L. Pegg, "ILAW PCT, VHT, Viscosity, and Electrical Conductivity Model Development," VSL-07R1230-1, Vitreous State Laboratory, The Catholic University of America, Washington, D.C., 2007.
 17. W. K. Kot, K. Klatt, and I. L. Pegg, "Glass Formulation to Support Melter Runs with HLW Simulants," Vitreous State Laboratory at The Catholic University of America, Washington, D.C., 2003.
 18. T. Sugawara, J. Katsuki, T. Shiono, S. Yoshida, J. Matsuoka, K. Minami, and E. Ochi, "High-temperature heat capacity and density of simulated high-level waste glass," *Journal of Nuclear Materials* **454** [1-3] 298-307 (2014).
 19. M. Schweiger, et al., "Expanded High-Level Waste Glass Property Data Development: Phase I," PNNL-17950, Pacific Northwest National Laboratory, Richland, WA, USA, 2011.
 20. B. J. Riley, B. T. Rieck, J. S. McCloy, J. V. Crum, S. K. Sundaram, and J. D. Vienna, "Tellurite glass as a waste form for mixed alkali-chloride waste streams: Candidate materials selection and initial testing," *Journal of Nuclear Materials* **424** [1] 29-37 (2012).
 21. J. Matyáš and R. Engler, "Assessment of Methods to Consolidate Iodine-Loaded Silver-Functionalized Silica Aerogel," PNNL-22874, Pacific Northwest National Laboratory, Richland, WA, 2013.

- 1
2
3
4
5
6
7
8
9
10
11
12
13
14
15
16
17
18
19
20
21
22
23
24
25
26
27
28
29
30
31
32
33
34
35
36
37
38
39
40
41
42
43
44
45
46
47
48
49
50
51
52
53
54
55
56
57
58
59
60
22. D. Ditmars, S. Ishihara, S. S. Chang, and G. Bernstein, "Enthalpy and heat-capacity standard reference material: synthetic sapphire (α -Al₂O₃) from 10 to 2250 K," *J. Res. Natl. Bur. Stand.* **87** [2] 159-163 (1982).
23. Gan, H., et al., "Crystal Settling, Redox, and High Temperature Properties of ORP HLW and LAW Glasses," Vitreous State Laboratory at The Catholic University of America, Washington, D.C., 2009.
24. M. M. Ammar, S. A. Gharib, M. M. Halawa, H. A. El-Batal, and K. El-Badry, "Thermal Conductivity of Silicate and Borate Glasses," *Journal of the American Ceramic Society* **66** [5] C-76–C-77 (1983).
25. N. P. Bansal and R. H. Doremus, *Handbook of glass properties*, Elsevier, 2013.
26. L. van der Tempel, G. P. Melis, and T. C. Brandsma, "Thermal Conductivity of a Glass: I. Measurement by the Glass–Metal Contact," *Glass Physics and Chemistry* **26** [6] 606-611 (2000).
27. S. Samal, J. Lee, D-Y Jeong, and H. Kim, "Characterization of thermal conductivity of SiO₂–Al₂O₃–Y₂O₃ glasses," *Thermochimica Acta* **604** 1-6 (2015).

Figure Captions

1
2
3 Figure 1. DSC curves of three empty crucibles (a) and comparison between three sapphire
4
5 measurements (b). The dashed curve represents the temperature profile used for the
6
7 measurements.
8

9
10 Figure 2. Heat capacity (C_p) curves of sapphire (from the heating segment) with the reference
11
12 sapphire values.
13

14 Figure 3. Heat capacity (C_p) curves of LAW simulated glasses from the cooling segment.
15

16
17 Figure 4. Heat capacity (C_p) curves of HLW simulated glasses from the cooling segment.
18

19 Figure 5. Heat capacity (C_p) curves of Sugawara glass compositions.
20

21 Figure 6. Density as a function of temperature up to 400°C.
22

23
24 Figure 7. Diffusivity of LAW (a) and HLW (b) glasses as a function of temperature, measured by
25
26 flash method.
27

28 Figure 8. Thermal conductivity of LAW (a) and HLW (b) glasses as a function of temperature.
29

30
31 Figure 9. Thermal conductivity of LAW (a) and HLW (b) glasses as a function of temperature,
32
33 compared with high temperature measurements (800–1150°C) by Gan et al.²³ (labeled “*” in the
34
35 key).
36

37
38 Figure 10. Comparison of measured C_p values to WTP Conservative LAW Baseline from 200 to
39
40 800°C.
41
42
43
44
45
46
47
48
49
50
51
52
53
54
55
56
57
58
59
60

1
2
3
4
5
6
7
8
9
10
11
12
13
14
15
16
17
18
19
20
21
22
23
24
25
26
27
28
29
30
31
32
33
34
35
36
37
38
39
40
41
42
43
44
45
46
47
48
49
50
51
52
53
54
55
56
57
58
59
60

For Peer Review

Table 1. Chemical composition (target wt.%) of the glasses used for the current study

Oxides	LAWA44	ORPLA20	ORPLD1	LAWB99	HLW- Ng- Fe2	HLW- E-Al- 27	WTP- C106	Sugawara A	Sugawara B
Al ₂ O ₃	6.20	6.70	10.16	10.15	5.58	23.97	4.89	5.10	4.93
Ag ₂ O	-	-	-	-	-	-	-	-	0.01
B ₂ O ₃	8.90	8.80	12.05	11.01	13.81	15.19	10.27	15.46	14.89
BaO	-	-	-	-	0.08	0.05	0.07	0.59	0.35
Bi ₂ O ₃	-	-	-	-	-	1.15	0.46	-	-
CaO	1.99	3.34	8.02	10.21	0.52	6.08	0.10	3.25	3.02
CdO	-	-	-	-	-	0.02	-	-	-
CoO	-	-	-	-	-	-	-	0.18	0.23
Cl	0.65	0.68	0.33	0.01	-	-	-	-	-
Ce ₂ O ₃	-	-	-	-	0.11	-	0.10	1.75	2.14
Cr ₂ O ₃	0.02	0.50	0.50	0.11	0.26	0.52	0.22	-	-
Cs ₂ O	-	-	0.13	-	-	-	-	0.00	0.90
F	0.01	-	0.17	0.07	-	0.67	-	-	-
Fe ₂ O ₃	6.98	0.30	1.00	1.15	16.01	5.90	14.03	0.92	1.11
Gd ₂ O ₃	-	-	-	-	-	-	-	1.66	0.36
K ₂ O	0.50	0.54	0.16	0.41	-	0.14	-	0.19	0.21
La ₂ O ₃	-	-	-	-	0.09	-	0.08	3.12	2.23
Li ₂ O	-	-	-	3.54	1.55	3.57	2.64	3.76	3.72
MgO	1.99	0.93	1.00	1.15	0.16	0.12	0.14	-	-
MnO	-	-	-	-	3.23	-	2.82	0.38	0.53
MoO ₃	-	-	-	-	-	-	-	0.00	0.05
Na ₂ O	20.01	24.00	21.00	10.00	14.17	9.58	12.55	10.07	10.49
Nd ₂ O ₃	-	-	-	-	-	-	-	0.00	1.81
NiO	-	-	0.04	-	0.47	0.40	0.41	0.60	0.61
P ₂ O ₅	0.03	-	0.29	0.03	0.64	1.05	0.56	-	-
Pr ₂ O ₃	-	-	-	-	-	-	-	0.40	0.57
PbO	-	-	0.01	-	0.62	0.41	0.54	-	-
Re ₂ O ₇	0.10	-	-	-	-	-	-	-	-
SiO ₂	44.57	42.51	37.17	43.08	41.05	30.50	47.75	47.45	46.45
Sm ₂ O ₃	-	-	-	-	-	-	-	0.00	0.04
SnO ₂	-	2.76	-	-	0.07	-	0.06	-	-
SO ₃	-	-	-	-	-	-	-	-	-
target	0.10	0.18	0.96	0.75	0.22	0.20	0.19	-	-
SrO	-	-	-	-	0.19	-	0.17	-	-
TeO ₂	-	-	-	-	-	-	-	0.00	0.02
TiO ₂	1.99	-	-	-	-	0.01	-	-	-
V ₂ O ₅	-	-	1.00	1.24	-	-	-	-	-
ZnO	2.96	2.76	3.00	3.54	0.03	0.08	1.03	0.03	0.03
ZrO ₂	2.99	6.00	3.00	3.54	1.13	0.40	0.98	2.28	2.33

Table 2. Summary of C_p , ρ , α , and k of the HLW glasses. Note that italic-bold values are extrapolations of C_p or diffusivity.

HLW-Ng-Fe2					HLW-E-Al-27				WTP-C106			
T °C	C_p J/kg·K	ρ kg/m ³	α m ² /s	k W/(m·K)	C_p J/kg·K	ρ kg/m ³	α m ² /s	k W/(m·K)	C_p J/kg·K	ρ kg/m ³	α m ² /s	k W/(m·K)
25	858.6	2719.4	4.30E-07	1.00	908.1	2544.1	4.60E-07	1.06	868.7	2703.9	4.40E-07	1.03
50	876.5	2717.6	4.30E-07	1.02	929.4	2542.4	4.50E-07	1.06	888.0	2701.9	4.30E-07	1.03
75	894.5	2715.8	-	-	950.6	2540.9	-	-	907.3	2700.3	-	-
100	912.4	2714.1	4.20E-07	1.04	971.9	2539.3	4.40E-07	1.09	926.6	2698.7	4.20E-07	1.05
125	930.4	2712.2	-	-	993.1	2537.6	-	-	945.9	2696.8	-	-
150	948.3	2710.4	4.00E-07	1.03	1014.4	2535.9	4.30E-07	1.11	965.2	2694.9	4.20E-07	1.09
175	966.3	2708.4	-	-	1035.7	2534.2	-	-	984.5	2693.0	-	-
200	982.7	2706.4	4.10E-07	1.09	1055.8	2532.3	4.20E-07	1.12	1003.6	2691.0	3.30E-07	-
225	1003.8	2704.4	-	-	1079.0	2530.5	-	-	1024.9	2688.9	-	-
250	1023.0	2702.3	4.00E-07	1.11	1100.7	2528.5	4.10E-07	1.14	1045.0	2686.8	4.00E-07	1.12
275	1040.0	2700.2	-	-	1121.8	2526.6	-	-	1064.1	2684.7	-	-
300	1055.4	2698.0	3.90E-07	1.11	1142.8	2524.5	4.00E-07	1.15	1078.7	2682.6	4.00E-07	1.16
325	1070.4	2695.8	-	-	1162.3	2522.5	-	-	1094.5	2680.4	-	-
350	1086.9	2693.5	3.90E-07	1.14	1181.4	2520.4	4.00E-07	1.19	1113.7	2678.2	3.90E-07	1.16
375	1106.8	2691.2	-	-	1202.5	2518.3	-	-	1136.2	2676.0	-	-
400	1135.1	2688.8	3.90E-07	1.19	1231.8	2516.0	3.90E-07	1.21	1167.6	2674.0	3.90E-07	1.22

Table 3. Summary of C_p , ρ , α , and k of the LAW glasses. Note that **italic-bold** values are extrapolations of C_p or diffusivity.

LAWB99					LAWA44				ORPLA20				ORPLD1			
T	C_p	ρ	α	k	C_p	ρ	α	K	C_p	ρ	α	k	C_p	ρ	α	k
°C	J/kg·K	kg/m ³	m ² /s	W/(m·K)	J/kg·K	kg/m ³	m ² /s	W/(m·K)	J/kg·K	kg/m ³	m ² /s	W/(m·K)	J/kg·K	kg/m ³	m ² /s	W/(m·K)
25	834.7	2674.4	5.20E-07	1.16	853.7	2683.6	4.90E-07	1.12	887.6	2706.5	4.20E-07	1.01	864.6	2597.3	4.20E-07	0.94
50	849.9	2672.6	5.50E-07	1.25	870.1	2681.3	4.90E-07	1.14	901.3	2704.2	4.20E-07	1.02	889.3	2595.0	4.30E-07	0.99
75	865.1	2670.9	-	-	886.5	2679.4	-	-	915.1	2702.0	-	-	913.9	2593.1	-	-
100	880.3	2669.2	5.40E-07	1.27	902.9	2677.3	4.90E-07	1.18	928.9	2699.9	4.10E-07	1.03	938.6	2591.0	4.30E-07	1.05
125	895.5	2667.3	-	-	919.3	2675.2	-	-	942.7	2697.5	-	-	963.3	2588.9	-	-
150	910.7	2665.4	5.30E-07	1.29	935.6	2673.0	4.00E-07	-	956.4	2695.2	3.80E-07	-	988.0	2586.7	5.10E-07	-
175	925.9	2663.4	-	-	952.0	2670.8	-	-	970.2	2692.8	-	-	1012.7	2584.5	-	-
200	940.5	2661.5	5.00E-07	1.25	966.0	2668.5	4.30E-07	-	979.2	2690.3	3.80E-07	-	1004.2	2582.2	4.10E-07	-
225	957.6	2659.4	-	-	984.7	2666.2	-	-	997.6	2687.8	-	-	1078.8	2580.0	-	-
250	974.2	2657.3	5.10E-07	1.32	1002.3	2663.8	4.80E-07	1.28	1015.4	2685.3	4.00E-07	1.09	1100.5	2577.6	4.20E-07	1.19
275	987.8	2655.1	-	-	1019.3	2661.4	-	-	1027.1	2682.7	-	-	1121.5	2575.2	-	-
300	1000.2	2653.0	5.00E-07	1.33	1035.6	2659.1	4.70E-07	1.29	1041.4	2680.2	3.90E-07	1.09	1142.6	2572.8	4.20E-07	1.23
325	1013.6	2650.7	-	-	1050.4	2656.6	-	-	1053.2	2677.5	-	-	1162.1	2570.3	-	-
350	1027.9	2648.4	4.90E-07	1.33	1066.2	2654.2	4.70E-07	1.33	1065.8	2675.0	3.90E-07	1.11	1181.2	2567.9	4.20E-07	1.27
375	1045.6	2645.9	-	-	1081.8	2651.6	-	-	1079.0	2672.2	-	-	1202.3	2565.3	-	-
400	1069.1	2643.5	4.90E-07	1.38	1099.3	2649.2	4.70E-07	1.37	1093.1	2669.7	3.90E-07	1.14	1231.4	2562.8	4.20E-07	1.33

Table 4. Summary of C_p , ρ , α , and k of the Sugawara A and B glasses

T °C	Sugawara A				Sugawara B			
	C_p J/kg·K	ρ kg/m ³	α m ² /s	K W/(m·K)	C_p J/kg·K	ρ kg/m ³	α m ² /s	k W/(m·K)
25	886.8	2729.8	4.70E-07	1.14	858.9	2739.9	4.30E-07	1.01
50	905.5	2727.9	4.60E-07	1.14	878.8	2738.0	4.20E-07	1.01
75	924.1	2726.3	-	-	898.6	2736.4	-	-
100	942.8	2724.7	4.50E-07	1.16	918.5	2734.7	4.10E-07	1.03
125	961.5	2722.8	-	-	938.4	2732.9	-	-
150	980.1	2721.0	4.40E-07	1.17	958.2	2731.0	4.00E-07	1.05
175	998.8	2719.1	-	-	978.1	2729.1	-	-
200	1014.1	2717.2	4.40E-07	1.21	992.9	2727.1	4.00E-07	1.08
225	1036.2	2715.2	-	-	1016.0	2725.1	-	-
250	1056.7	2713.2	4.30E-07	1.23	1039.2	2723.1	3.90E-07	1.10
275	1074.2	2711.1	-	-	1060.5	2720.9	-	-
300	1091.5	2709.0	4.30E-07	1.27	1080.4	2718.8	3.80E-07	1.12
325	1110.8	2706.8	-	-	1098.0	2716.5	-	-
350	1128.9	2704.7	4.20E-07	1.28	1115.0	2714.3	3.80E-07	1.15
375	1148.3	2702.4	-	-	1133.8	2711.9	-	-
400	1170.7	2700.1	4.20E-07	1.33	1156.0	2709.6	3.80E-07	1.19

Note: Data are not complete at the time of this report.

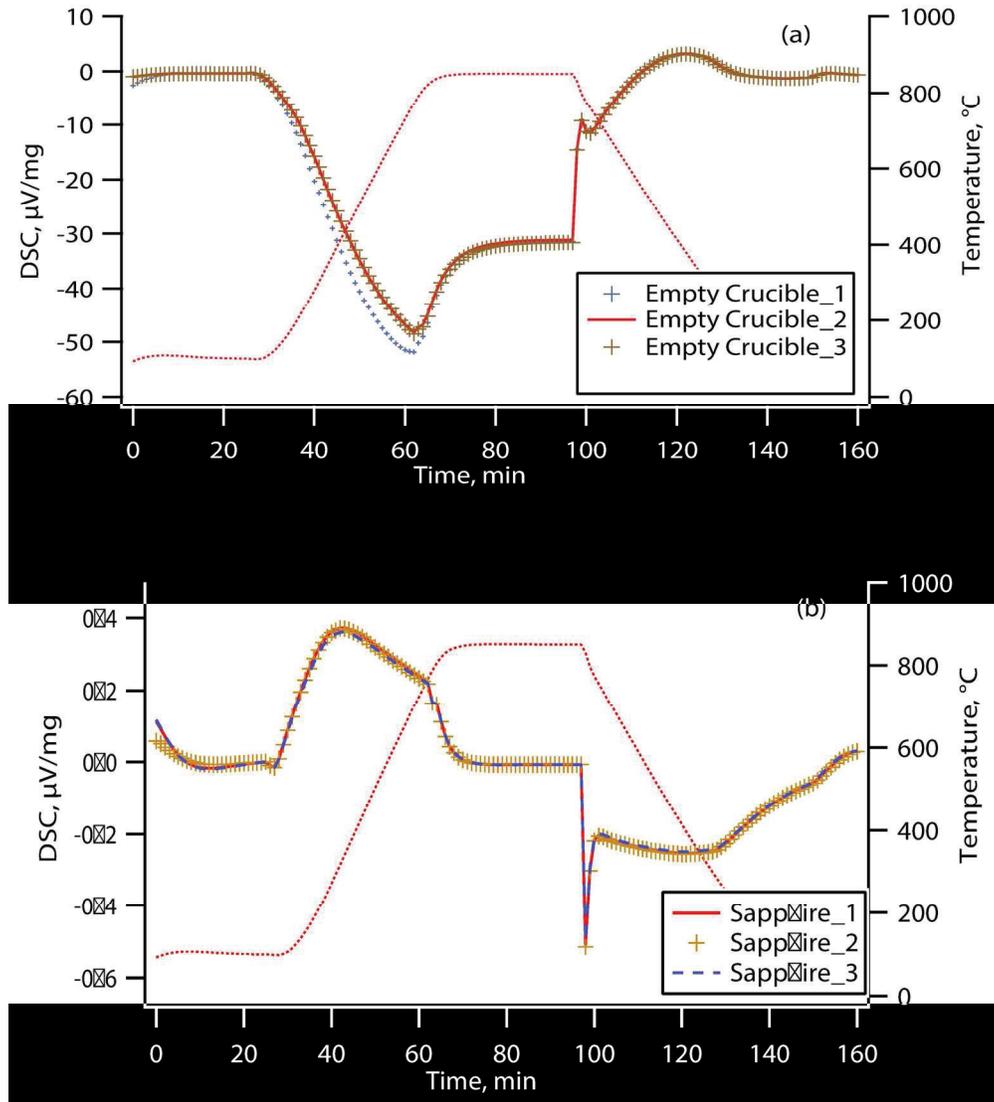


Figure 1. DSC curves of three empty crucibles (a) and comparison between three sapphire measurements (b). The dashed curve represents the temperature profile used for the measurements.
159x176mm (300 x 300 DPI)

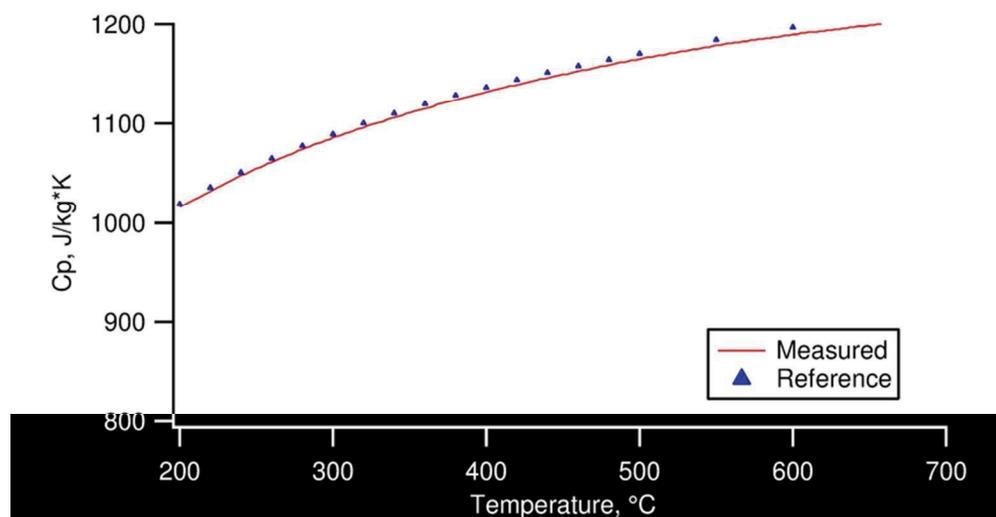


Figure 2. Heat capacity (C_p) curves of sapphire (from the heating segment) with the reference sapphire values
72x38mm (300 x 300 DPI)

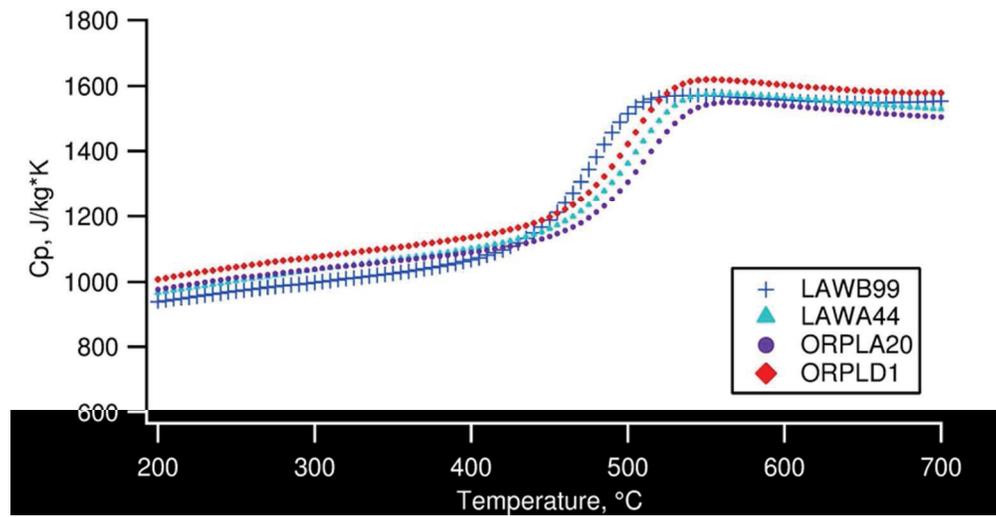


Figure 3. Heat capacity (C_p) curves of LAW simulated glasses from the cooling segment 72x38mm (300 x 300 DPI)

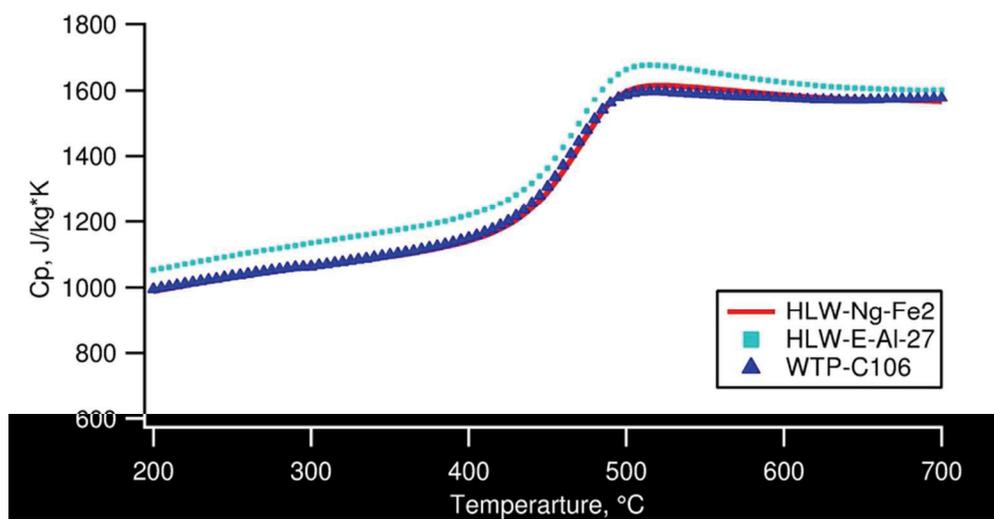


Figure 4. Heat capacity (C_p) curves of HLW simulated glasses from the cooling segment 72x38mm (300 x 300 DPI)

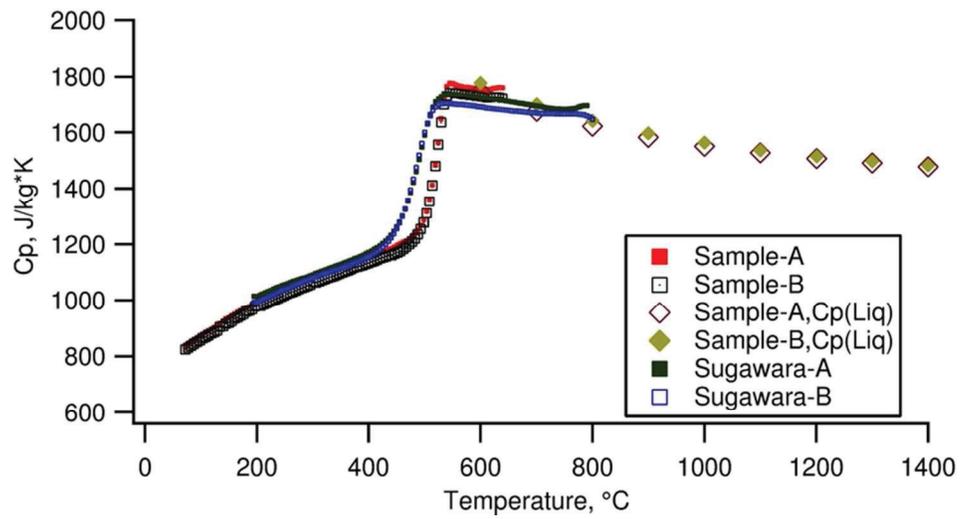


Figure 5. Heat capacity (Cp) curves of Sugawara glass compositions 72x38mm (300 x 300 DPI)

Peer Review

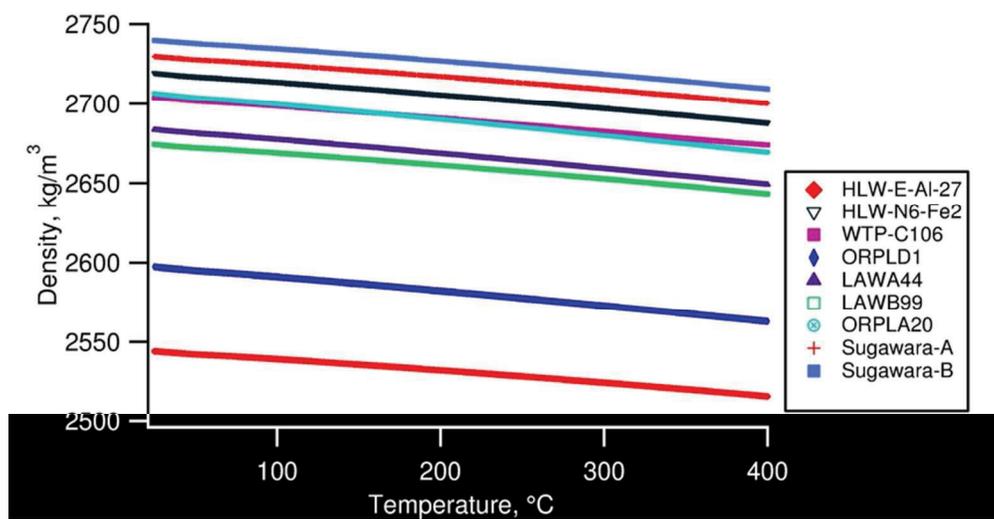


Figure 6 . Density as a function of temperature up to 400°C
72x38mm (300 x 300 DPI)

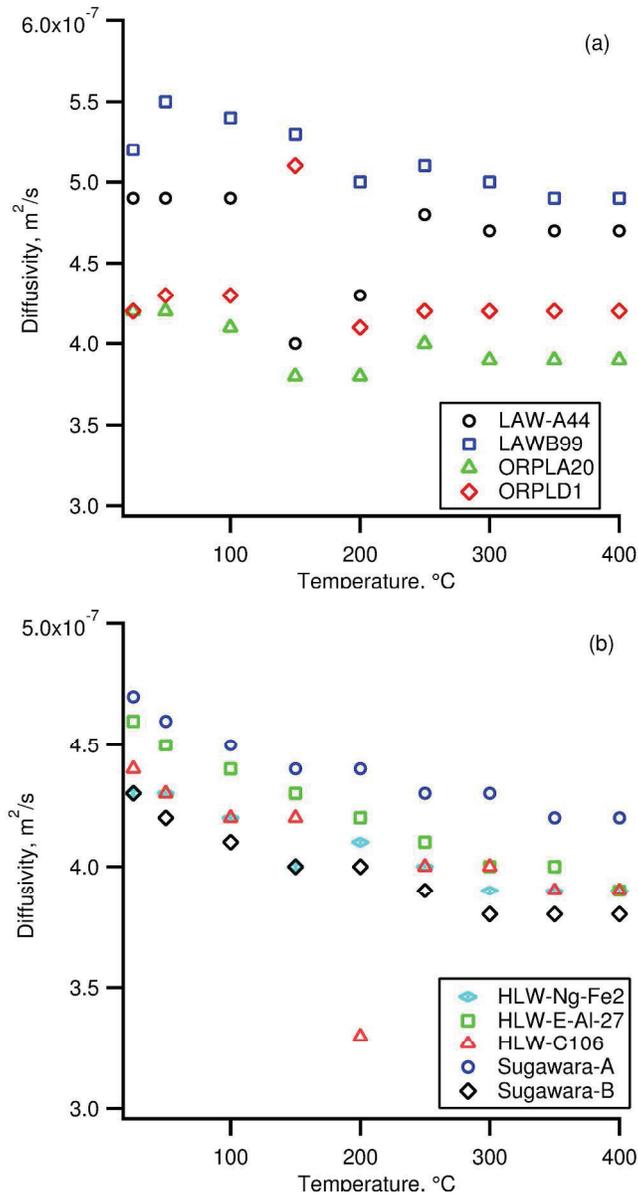


Figure 7. Diffusivity of LAW (a) and HLW (b) glasses as a function of temperature, measured by flash method.

196x354mm (300 x 300 DPI)

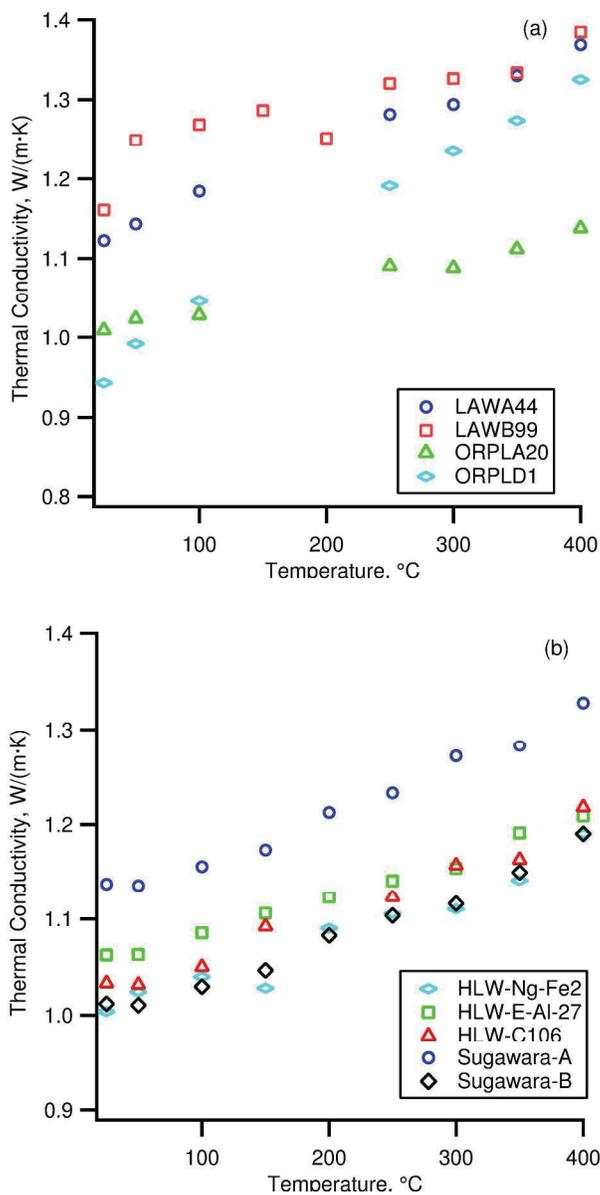


Figure 8. Thermal conductivity of LAW (a) and HLW (b) glasses as a function of temperature. 200x383mm (300 x 300 DPI)

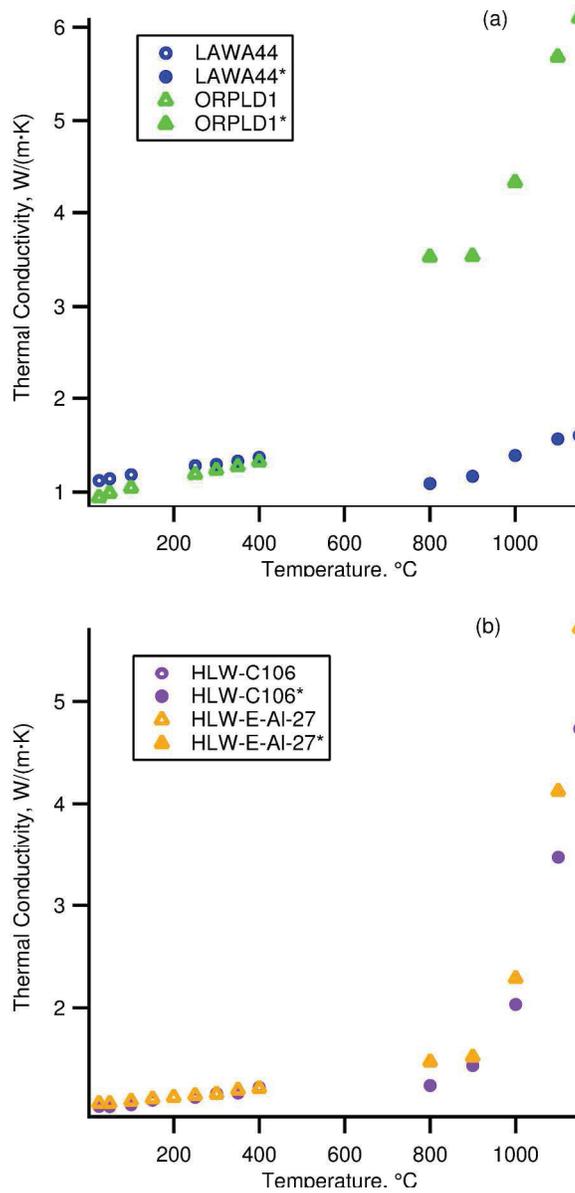


Figure 9. Thermal conductivity of LAW (a) and HLW (b) glasses as a function of temperature, compared with high temperature measurements (800–1150°C) by Gan et al.²³ (labeled "*" in the key).
199x385mm (300 x 300 DPI)

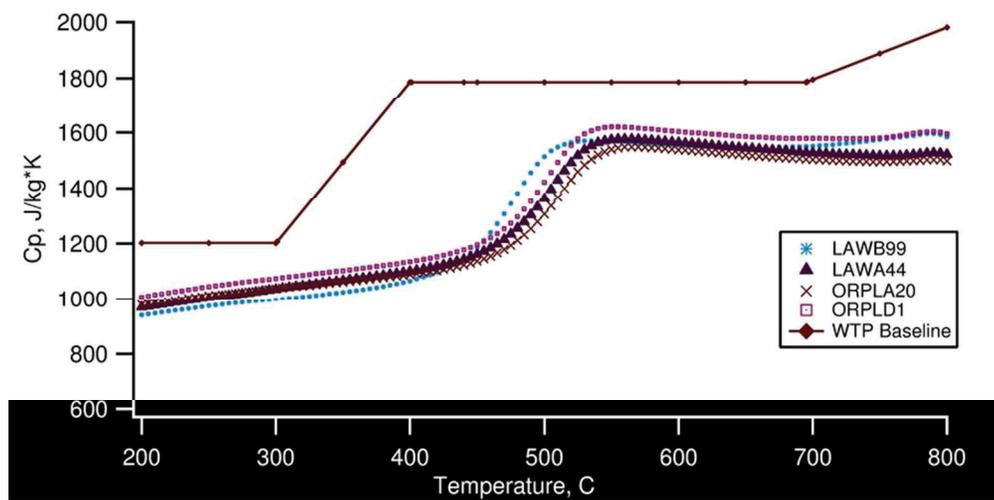


Figure 10. Comparison of measured C_p values to WTP Conservative LAW Baseline from 200 to 800°C
76x38mm (300 x 300 DPI)